Meteorology and Atmospheric Physics, Volume 132, April 2020, pp. 73–285
DOI:10.1007/s00703-019-00689-2

CFD simulation of dense gas dispersion in neutral atmospheric boundary layer with OpenFOAM

Vu Tran · E. Y. K. Ng · Martin Skote

Received: date / Accepted: date

Abstract In this study, MOST (Monin-Obukhov Similarity Theory) is used to specify the profiles of velocity, turbulent kinetic energy (k) and eddy dissipation rate (ϵ) in ABL (Atmospheric Boundary Layer) flow. The OpenFOAM standard solver *buoyantSimpleFoam* is modified to simulate neutrally stratified ABL. The solver is able to obtain equilibrium ABL. For gas dispersion simulation, *buoyantNonReactingFoam* is developed to take into accounts fluid properties change due to temperature, buoyancy effect and variable turbulent Schmidt number. The solver is validated for dense gas dispersion in wind tunnel test and field test of LNG (Liquefied Natural Gas) vapour dispersion in neutrally stratified ABL.

Keywords LNG dispersion · CFD · ABL · OpenFOAM

Vu Tran, E. Y. K. Ng

School of Mechanical and Aerospace Engineering, Nanyang Technological University, Singapore

E-mail: tranlevu001@e.ntu.edu.sg

Martin Skote

School of Aerospace, Transport and Manufacturing, Cranfield University, UK

1 Introduction

Many human activities are affected by the atmospheric boundary layer (ABL). This is also where most air pollution phenomena occur. Understanding of the processes taking place in the ABL has attracted various research studies. Some typical applications of ABL related research topics are wind engineering, urban flows, weather forecast, air pollution and risk assessment of hazardous material spills in industrial sites

One hazardous dense gas is liquefied natural gas (LNG), which is an effective solution for long-distance natural gas transfer. LNG has become the preferred option for international trading of natural gas. However, LNG storage, handling, transportation are exposed to serious risks for humans, equipment and the environment due to thermal hazards associated with combustion events such as pool fire, vapour cloud fire, explosion or rapid phase transition. Safety assessment and hazard mitigation methods should be applied to lower the possibilities of catastrophic disaster relating to the LNG industry. The scope of this study is constrained to the discussion of dense gas dispersion when released into the ABL.

Computational Fluid Dynamics (CFD) is increasingly being used in simulation of ABL flows. Open source CFD tool is a more powerful research tool in comparison to proprietary software because of its flexibility to incorporate new implementation of fields calculation and post-processing. OpenFOAM is an open source CFD software package that attracts users from both industry and academia. Using a general CFD code such as OpenFOAM for simulating ABL flow and gas dispersion also encourages research sharing and reusing code in this specific field where in-house code is usually adopted.

An important task before modelling gas dispersion in the ABL is obtaining the crrect ABL flow prior to the release of gas source. One approach to achieve this is using equilibrium ABL, i.e. zero stream-wise gradients of all variables, as a steady state ABL flow. For neutral ABL, Richards and Hoxey (1993) proposed appropriate boundary conditions of mean wind speed and turbulence quantities for the standard $k-\epsilon$ model based on Monin-Obukhov similarity theory (MOST). These profiles were derived assuming constant shear stress with height and were used to model ABL as horizontally homogeneous turbulent surface layer (HHTSL). However, HHTSL was hard to achieve mostly due to the ground boundary conditions (Yang et al., 2009), which manifested in a decay of velocity profile due to a spike in the turbulent kinetic energy close to the ground. However, consistency between wall boundary conditions, turbulence model with associated constants and numerical schemes was shown to achieve HHTSL (Jonathon and Christian, 2012; Parente et al., 2011; Yan et al., 2016). These authors adopted proprietary CFD software for their simulation. Applying these implementations in open-source CFD code also require extensive modifications of the source code to successfully simulate equilibrium ABL. OpenFOAM was previously used for atmospheric buoyant (Flores et al., 2013) and dense gas dispersions (Mack and Spruijt, 2013; Fiates et al., 2016; Fiates and Vianna, 2016). However, the validation of these solvers in simulation of equilibrium ABL was not reported. Therefore, the atmospheric turbulence might not be correctly solved throughout the computational domain.

In this study, MOST is used to model the profiles of velocity, turbulent kinetic energy (k) and eddy dissipation rate (ϵ) of ABL according to an approach proposed by Richards and Hoxey (1993). These profiles are used as the boundary conditions at the inlet of ABL flow simulation. OpenFOAM application `buoyantSimpleFoam`

is modified to simulate neutrally stratified ABL turbulence. For gas dispersion simulation, `buoyantNonReactingPimpleFoam` is developed to take into account the buoyancy effect and variable turbulent Schmidt number. The solver is validated for dense gas dispersion cases from wind tunnel and field tests of LNG vapour dispersion in neutrally stratified ABL.

2 Methodology

2.1 Models

The $k-\epsilon$ model is used for turbulence modelling. It is based on expression of turbulent dynamic viscosity μ_t by Jones and Launder (1972):

$$\mu_t = \rho C_\mu \frac{k^2}{\epsilon} \tag{1}$$

Two additional transport equations for turbulence kinetic energy k and turbulence dissipation rate ϵ are required. To include the effect of buoyancy, the transport equations for k and ϵ are:

$$\frac{D}{Dt}(\rho k) = \frac{\partial}{\partial x_i}\left[\left(\mu + \frac{\mu_t}{\sigma_k}\right)\frac{\partial k}{\partial x_j}\right] + G_k + G_b - \rho\epsilon \tag{2}$$

$$\frac{D}{Dt}(\rho \epsilon) = \frac{\partial}{\partial x_i}\left[\left(\mu + \frac{\mu_t}{\sigma_\epsilon}\right)\frac{\partial \epsilon}{\partial x_j}\right] + C_{1\epsilon}\frac{\epsilon}{k}G_k + C_{1\epsilon}C_{3\epsilon}\frac{\epsilon}{k}G_b - C_{2\epsilon}\rho\frac{\epsilon^2}{k} \tag{3}$$

where ρ is the fluid density; $C_\mu = 0.09$, $\sigma_k = 1$, $\sigma_\epsilon = 1.3$, $C_{1\epsilon} = 1.44$ and $C_{2\epsilon} = 1.92$ are model constants as proposed in original paper (Launder and Spalding, 1974). The value of $C_{3\epsilon}$ is calculated using:

$$C_{3\epsilon} = tanh \left| \frac{v}{u} \right| \tag{4}$$

where v, u are vertical and horizontal velocity accordingly.

G_k is production of turbulence kinetic energy due to the mean velocity gradients. G_b is the buoyancy source term:

$$G_b = -\frac{\mu_t}{\rho Pr_t}(\boldsymbol{g} \cdot \boldsymbol{\nabla}\rho) = -C_g \frac{\mu_t}{\rho}(\boldsymbol{g} \cdot \boldsymbol{\nabla}\rho) \tag{5}$$

where $C_g = 1/Pr_t$ is used as a model constant to take into account the user-defined value of turbulent Prandtl number Pr_t. $\boldsymbol{g}$ is gravitational vector.

Energy, heat and transport properties are determined by a set of thermophysical models (Greenshields, 2017) in OpenFOAM. This set defines mixture type, transport and thermodynamic properties models, choice of energy equation variable and equation of states.

The fluid in a simulation is defined as a mixture of fixed compositions. Enthalpy is chosen as energy equation variable. Transport and thermodynamic properties are determined using models based on the density ρ, which are calculated from pressure and temperature fields. Polynomial functions of order N are used to relate transport property μ, the specific heat c_p and density ρ with temperature field T:

$$\begin{aligned} \mu &= \sum_{i}^{N-1} a_{\mu i} T^i \\ c_p &= \sum_{i}^{N-1} a_{c_p i} T^i \\ \rho &= \sum_{i}^{N-1} a_{\rho i} T^i \end{aligned} \tag{6}$$

where $a_{\mu i}$, $a_{c_p i}$ and $a_{\rho i}$ are the polynomials coefficients.

2.2 Boundary conditions

2.2.1 ABL air inlet

MOST ha been validated for the surface layer of ABL by many empirical studies (Foken, 2006). It assumes horizontally homogeneous and quasi-stationary flow field, i.e. profiles of flow variables are only varying in the vertical direction and their vertical fluxes are assumed constant. The inlet boundary conditions proposed by Richards and Hoxey (1993) based on MOST are widely used in CFD study of atmospheric flow. The velocity, turbulent production rate k and dissipation rate ϵ profiles in vertical direction z are written as:

$$\begin{aligned} u(z) &= \frac{u_*}{\kappa} \ln \frac{z + z_0}{z_0} \\ k &= \frac{u_*^2}{\sqrt{C_\mu}} \\ \epsilon(z) &= \frac{u_*^3}{\kappa(z + z_0)} \end{aligned} \tag{7}$$

where z_0 is aerodynamic roughness length, u_* is friction velocity, C_μ is $k - \epsilon$ model constant.

These profiles are implemented in OpenFOAM as `atmBoundaryLayer` class and its subclasses. Required parameters are flow and vertical direction, reference velocity, reference height and aerodynamic roughness length. The friction velocity is calculated as:

$$u_* = \frac{\kappa * u_{ref}}{\ln((z_{ref} + z_0)/z_0)} \tag{8}$$

Parente et al. (2011) presented an elaborate procedure to ensure the consistency for arbitrary inlet profile of turbulent kinetic energy k. Instead of altering model

constants as Yang et al. (2009), the effect of non-constant k on momentum and ϵ equation can be characterised by deriving an equation for C_μ:

$$C_\mu(z) = \frac{u_*^4}{k(z)^2} \tag{9}$$

Source terms are added to k and ϵ transport equations to ensure equilibrium condition:

$$\begin{aligned} S_k &= \frac{\rho u_* \kappa}{\sigma_k} \frac{\partial}{\partial z}\left((z+z_0)\frac{\partial k}{\partial z}\right) \\ S_\epsilon &= \frac{\rho u_*^4}{(z+z_0)^2}\left[\frac{(C_{\epsilon 2}-C_{\epsilon 1})\sqrt{C_\mu}}{\kappa^2} - \frac{1}{\sigma_\epsilon}\right] \end{aligned} \tag{10}$$

Richards and Norris (2011) revisited the problem of modelling the HHTSL by deriving the inlet profiles directly from the conservation and equilibrium equations. This allows various inlet profiles to be specified by varying the turbulence model constants. For standard $k-\epsilon$ models, the inlet profiles of velocity and turbulence properties are identical to Equation (7). However they suggested to change the von-Karman constant κ according to model constants as:

$$\kappa = \sqrt{(C_{\epsilon 2}-C_{\epsilon 1})\sigma_\epsilon \sqrt{C_\mu}} \tag{11}$$

Using the standard $k-\epsilon$ model constants, we obtain $\kappa_{k-\epsilon} = 0.433$.

2.2.2 Wall boundary conditions

In CFD, the below approximation is used to calculate wall shear stress:

$$\tau_w = \nu_t \frac{\partial u}{\partial n}|_w \approx \nu_t \frac{(u_P - u_w)}{y_P} \tag{12}$$

where y_P is distance to wall of the wall adjacent cell. Subscript w and P denote field value evaluated at wall and wall adjacent point respectively.

However, this approximation is inaccurate when wall velocity gradient is significantly larger than velocity difference between the adjacent cell and the wall. This is the case for most ABL flows. Turbulent kinematic viscosity ν_t wall function is used to calculate the wall shear stress τ_w from the wall velocity difference. To take into account the aerodynamic roughness length z_0, the calculation of turbulent kinematic viscosity at wall adjacent cell is:

$$\nu_t = \frac{\kappa u_* y_P}{\ln\left(\frac{y_P + z_0}{z_0}\right)} \tag{13}$$

where friction velocity u_* can be calculated from a simple relation derived by Launder and Spalding (1974), assuming that generation and dissipation of energy are in balance:

$$u_* = C_\mu^{1/4} k^{1/2} \tag{14}$$

ϵ wall function is used to calculate value of ϵ at wall adjacent cell ϵ_P as:

$$\epsilon_P = \frac{C_\mu^{0.75} k^{1.5}}{\kappa y_P + z_0} \tag{15}$$

The wall is usually defined as non-slip condition where velocity is zero. However, to account for the effect of aerodynamic roughness length, a new boundary condition for velocity is implemented in OpenFOAM as:

$$u_P = \frac{u_*}{\kappa} \ln\left(\frac{y_P + z_0}{z_0}\right) \tag{16}$$

2.2.3 Top, side and outlet boundaries

At the outlet boundary, the flow is assumed fully developed and unidirectional. All flow variables are supposed to be constant at this boundary.

The top and side of the computational domain are external boundaries representing the far fields of flow. If a constant pressure is applied in these boundaries, this may alter the inlet wind profile in case the prescribed pressure is not matched with the boundary velocity (Luketa-Hanlin et al., 2007). The zero gradient boundary condition, which set normal velocity to zero and all others variables are set equal to the inner values, or symmetry condition can be used at the top and side boundaries to reserve the wind profile and eliminate the effect of changing the inlet profiles.

Hargreaves and Wright (2007) showed that zero gradient velocity at the top boundary resulted in a decay of velocity downstream, due to the extraction of energy at the wall with respect to the wall shear stress. A driving shear stress, zero flux of turbulent kinetic energy and a flux of dissipation rate ϵ are imposed at the upper boundary:

$$\begin{aligned} \frac{du}{dz} &= \frac{u_*}{\kappa z} \\ \frac{\mu_t}{\sigma_\epsilon}\frac{d\epsilon}{dz} &= -\frac{\rho u_*^4}{\sigma_\epsilon z} \end{aligned} \tag{17}$$

2.3 Numerical tool and data sets

OpenFOAM is an open source CFD software package based on finite volume method, co-located variables and unstructured polyhedral meshes. In this study, `buoyantSimpleFoam` is used to simulate ABL turbulence. The application `buoyantNonReactingFoam`

is developed based on `rhoReactingBuoyantFoam` solver, previously used for dense gas dispersion by Fiates et al. (2016), to simulate atmospheric turbulence under neutral stability for dispersion of dense gas continuous source in flat terrain. `buoyantNonReactingFoam` uses polynomial thermophysical models to account for the change of fluid properties due to temperature. The solver takes into account the buoyancy effect and the variable turbulent Schmidt number. Algorithms used in these two solvers are presented in Algorithm 1 and 2.

Algorithm 1 `buoyantSimpleFoam` solver algorithm

1: Initializing variables such as: time variables, mesh, solution control, fields and continuity errors
2: **while** $t < t_{end}$ **do**
3: Solving momentum equation
4: Solving energy equation for enthalpy and correcting thermal properties
5: Solving pressure correction equation for p_{rgh} and calculating pressure field
6: Correcting turbulent properties
7: Writing fields
8: **end while**

Algorithm 2 `buoyantNonReactingFoam` solver algorithm

```
Initializing variables such as: time variables, mesh, solution control, fields and continuity errors
while t < t_end do
    t+ = Δt
    Solving continuity equation for density
    while PIMPLE outer correctors do
        Solving momentum equation
        Solving species transport equation
        Solving energy equation for enthalpy and correcting thermal properties
        while PIMPLE inner correctors do
            Solving pressure correction equation for p_rgh and calculating pressure field
            Solving continuity equation for density
            Calculating time step continuity errors
        end while
        Correcting turbulent properties
    end while
    Writing fields
end while
```

Boundary conditions used for ABL flows are developed as new libraries in OpenFOAM. These include velocity inlet, turbulent kinetic energy, dissipation rate inlet and wall boundary conditions.

A set of full scale field tests and experimental wind tunnel tests for LNG dispersion model validation was reported in (Ivings et al., 2013). Most data of these tests were available in REDIPHEM database (Nielsen and Ott, 1996). The data contains physical comparison parameters of each test. These are maximum arc-wise concentration, i.e. the maximum concentration across an arc at the specified

distance from the source and point-wise concentration, i.e. the concentration at specific sensor locations. Two wind tunnel data `DA0120` and `DAT223` are used to validate OpenFOAM solver in prediction of dense gas dispersion over a flat, unobstructed terrain in simulated neutral ABL. In these tests, continuous source of SF_6 gas was released in flat terrain without obstructions. For field test, we select `Burro9`, which is continuous LNG spills under neutral ABL.

3 Neutral ABL simulation

3.1 Domain and mesh

A 2D domain of 5000 m $\times$ 500 m with the resolution of 500 $\times$ 50 cells is used for the simulation of neutral ABL over flat terrain. The mesh is uniform in stream-wise direction and stretched in vertical direction with the expansion ratio of 1.075.

3.2 Numerical setting

The boundary conditions of the cases are represented in Table 1.

Table 1 Boundary conditions for neutral ABL simulation

ABL inlet	profiles of k, u, ϵ	Eq. (7)
ABL outlet	`zeroGradient` for all variables	
	`fixedValue` for static pressure	
ABL side	`zeroGradient` for all variables	
ABL top	`zeroGradient` for all variables	
	`fixedFlux/zeroGradient` for u and ϵ	Eq. (17)
ABL bottom	`noSlip` for u	

ABL parameters used to define inlet variable profiles are listed in Table 2 according to the reference case of Hargreaves and Wright (2007):

Table 2 ABL parameters using for neutral ABL simulation

u_* (m/s)	z_0 (m)	u_{ref} (m/s)	z_{ref} (m)
0.625	0.01	10	6

Steady state simulation is employed using `buoyantNonReactingSimpleFoam` described in previous section. OpenFOAM discretisation schemes, velocity-pressure coupling algorithm as well as linear solvers are listed below:

- Time schemes: `steadyState`
- Gradient schemes: `Gauss linear`
- Divergence schemes: `Gauss limitedLinear 1`
- Surface normal gradient schemes: `corrected`
- Laplacian schemes: `Gauss linear corrected`
- Interpolation schemes: `linear`
- Solving algorithm: `SIMPLE`
- Linear solver for p: `GAMG` with `DICGaussSeidel` preconditioner
- Linear solver for U, h, k, epsilon: `PBiCGStab` with `DILU` preconditioner

Residual control is set at three order of magnitude for pressure and four order of magnitude for other variables such as U, k, ϵ and h. Modification of $k-\epsilon$ (Equation (11)) are used to simulate neutral ABL and comparing with standard models. These three cases are summarised in Table 3

Different levels of inlet kinetic energy are obtained by altering C_μ according to Equation (9). The source term by Pontiggia et al. (2009) is implemented us-

Table 3 Turbulence models setting for neutral ABL simulation

Turbulence model	`standard` $k-\epsilon$	
	`modified` $k-\epsilon$	Eq. (10)
Wall functions	`nutkWallFunction` for ν_t	
	`epsilonWallFunction` for ϵ	
	`kqRWallFunction` for k	

ing Equation (10). Two values of default value $C_\mu = 0.09$ and $C_\mu = 0.017$ are simulated and compared with Monin-Obukhov theory.

3.3 Results and discussion of neutral ABL simulations

Modification of $k-\epsilon$ models achieve the matched results as shown in Figure 1. Including source terms as in Equation (10) is sufficient to compensate terms deflection from calculation of von-Karman constant $\kappa_{k-\epsilon} = 4.3$ from model constants (Equation (11)) and $\kappa = 4.1$ used in Monin-Obukhov theory.

Results from modelling different turbulence kinetic energy by varying C_μ are presented in Figure 2. The profiles of velocity and dissipation rate are perfectly matched with the Monin-Obukhov profiles. In the $C_\mu = 0.017$ simulation, the value of k near ground is smaller than the theoretical value, however, the kinetic energy level is matched with the theory at greater height. The smaller value of k at the wall adjacent cell is due to the wall function, where wall treatment used with the default $C_\mu = 0.09$ is implemented. However, the overall results are acceptable for verifying the proposed model in simulating different levels of kinetic energy.

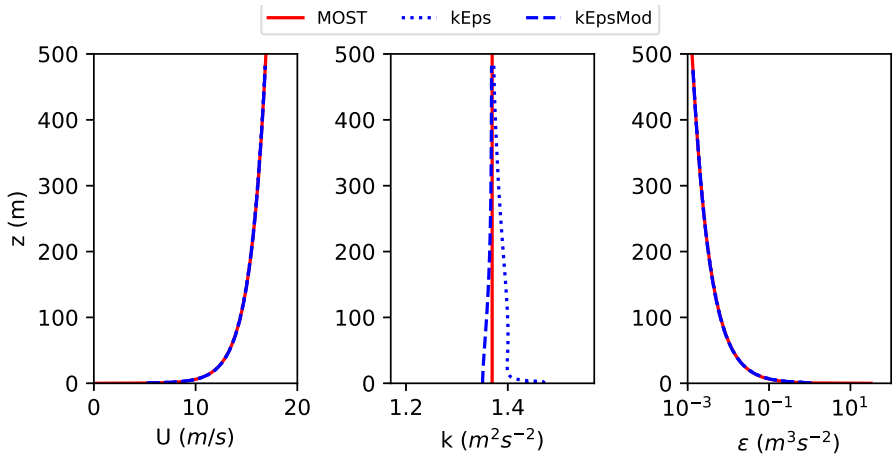

Fig. 1 Comparing velocity, turbulent kinetic energy and turbulent dissipation rate profiles at the outlet boundary from simulation of neutral ABL using standard $k-\epsilon$ (kEps), modified $k-\epsilon$ (kEpsMod) turbulence model and MOST inlet profiles (MOST)

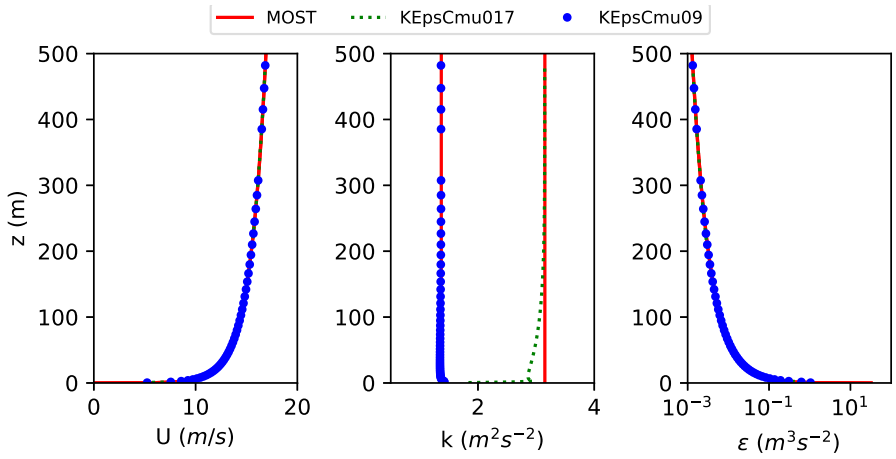

Fig. 2 Comparing velocity, turbulent kinetic energy and turbulent dissipation rate profiles from simulations of different kinetic energy levels by varying $C_\mu = 0.09$ (KEpsCmu09) $C_\mu = 0.017$ (KEpsCmu017) and MOST inlet profiles (MOST)

4 Dense gas dispersion in wind tunnel tests

4.1 Numerical setting

The effect of the turbulent Schmidt number Sc_t is investigated in dense gas dispersion. Three test cases are summarised in Table 4. The effect of turbulent models is examined by applying the modified $k-\epsilon$ which is already validated in simulating ABL over flat terrain in Section 3.

Table 4 Turbulent Schmidt number Sc_t in Hamburg tests

	Case 1	Case 2	Case 3
Sc_t	1	0.7	0.3
Label (Fig. 4, 10)	FOAM_ORIG	FOAM_Sc07	FOAM_Sc03

Firstly, the steady simulation using `bouyantSimpleFoam` is performed to establish the steady ABL flow prior to the dense gas release. The solver which includes buoyancy effects `bouyantSimpleFoam` is used to account for of density stratification in dense gas flow. The atmospheric inlet profiles are specified by MOST with parameters in Table 5. Standard $k-\epsilon$ with modifications is used to study the ability to simulate the ABL with each model. Secondly, the transient simulation is performed using steady simulation solutions as initial fields. A modified version of `rhoReactingBouyantFoam` is studied to model multi-species flow where mixture considered are air and dense gas SF_6. The wind tunnel tests were conducted in isothermal condition, therefore constant thermal and transport properties are used for both gases.

Table 5 Hamburg flat, unobstructed test case parameters (Nielsen and Ott, 1996)

	Unit	DA0120	DAT223
Substance		SF_6	SF_6
Density	kg/m^3	6.27	6.27
z_0	m	0.0001	0.0001
Wind speed	m/s	0.54	0.74
Reference height	m	0.00718	0.01367
Ambient temperature	^0C	20	20
Source diameter	m	0.07	0.07
Spill rate	kg/s	0.0001743	0.000872

In simulations of `DA0120` and `DAT223` tests, the discretisation schemes and linear solver setting are identical to the simulation of neutral ABL (Section 3).

4.2 Results and discussion of gas dispersion in wind tunnel tests

4.2.1 Peak concentration prediction

The steady state plumes at ground level of `DAT0120` and `DAT223` tests are plotted in Figure 3. Under higher release volume flow rate and higher wind speed, `DAT223` plume is wider and is spreading further downstream than the `DAT0120` plume.

The predicted and measured peak gas concentration are compared at several distances from the spill in Figure 4. Turbulent Schmidt number Sc_t has significant effect in predicting dense gas dispersion. The original `rhoReactingBouyantFoam` code, with assumption of species diffusivity equals to viscosity, is shown to over-predict concentration with a factor of three. The modified code takes into account the variable species diffusivity Sc_t by reading this parameter from user input. The

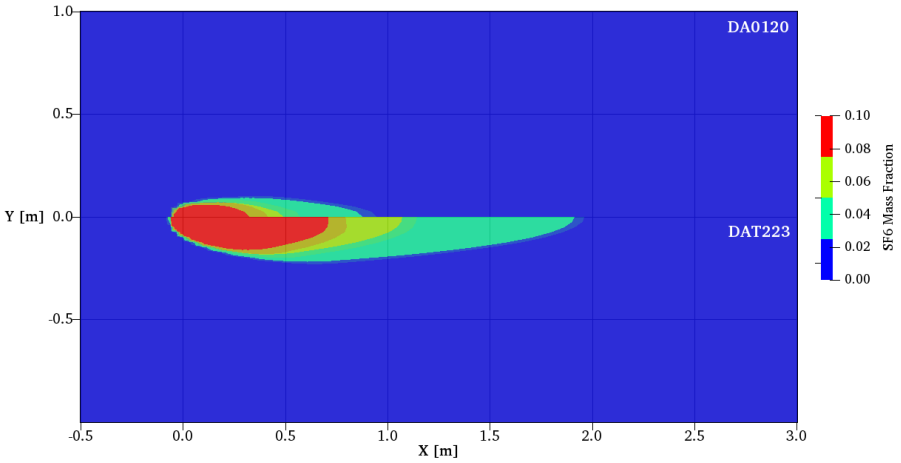

Fig. 3 `DA0120`(up) and `DAT223`(below) ground level contours of SF_6 mass fraction

value of $Sc_t = 0.3$ is shown to yield a perfect match with the experimental data. However, there is a slightly acceptable over-predicted species concentration at a point near the source release.

Results from the `DAT223` simulation are presented in Figure 5. Satisfactory over predicted peak concentration is similar to `DA0120` case.

4.2.2 Point-wise concentration

Figure 6 presents gas concentration at the downwind distance $X = 1.84$ of the `DA0120` test. The simulation can reproduce the averaged gas concentration. The first incidence time of gas concentration is earlier than observed in experiments. However, the time for reaching averaged maximum concentration is well predicted.

4.2.3 Statistical model evaluation

Statistical Performance Measures (SPMs) are means to compare prediction parameters and the measured ones for model evaluation. The SPM chosen should reflect

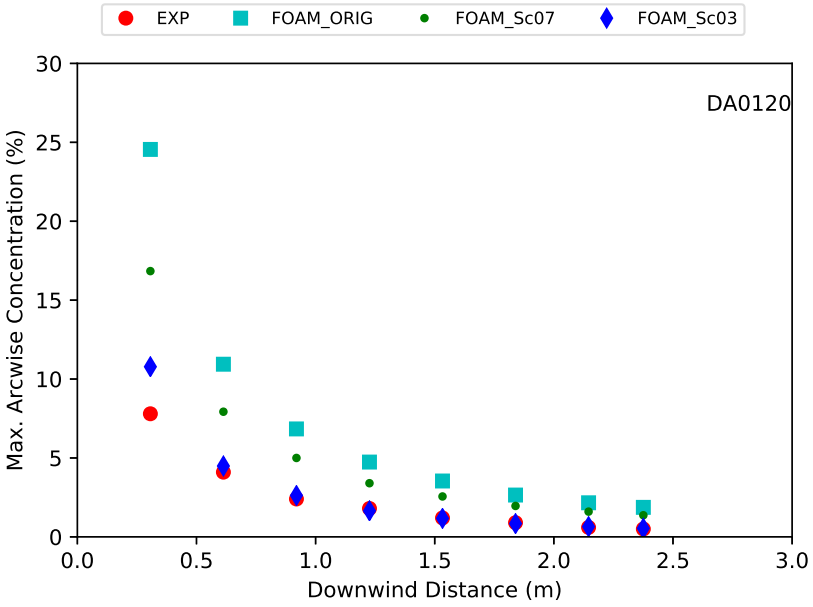

Fig. 4 Peak concentration for `DA0120` test

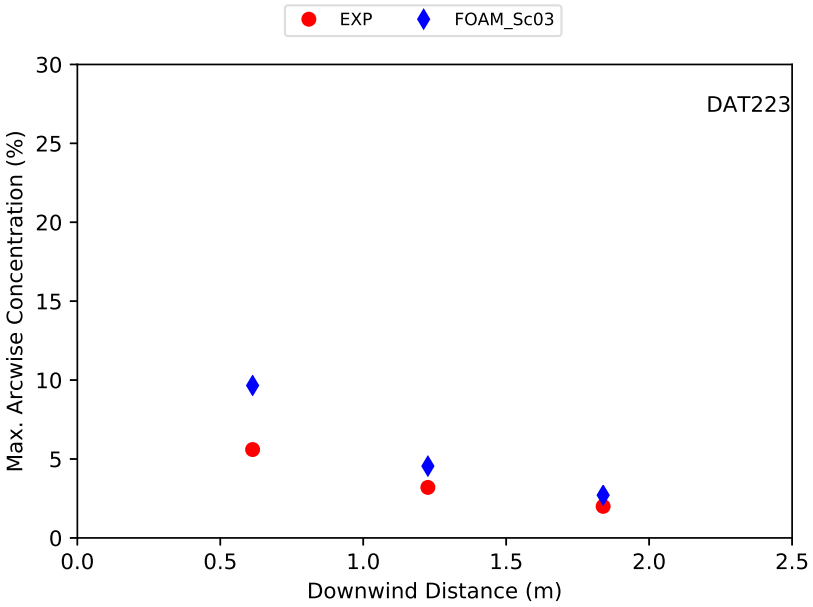

Fig. 5 Peak concentration for `DAT223` test

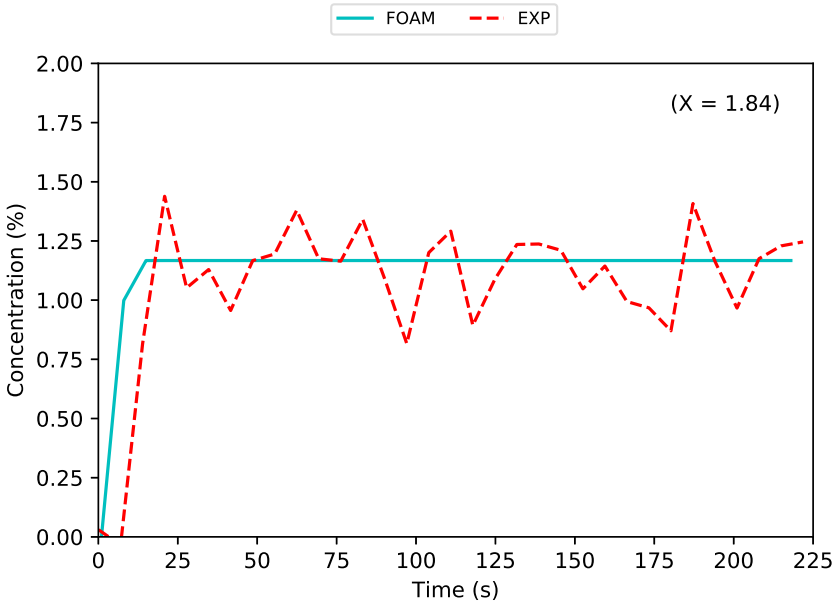

Fig. 6 Concentration at $X = 1.84$ of `DA0120` test

the bias of these predictions. In the context of LNG vapour dispersion model evaluation, Ivings et al. (2013) proposed five SPMs including mean relative bias (MRB), mean relative square error (MRSE), the fraction of predictions within the factor of two of measurements (FAC2), geometric mean bias (MG) and geometric variance (VG). Definition and acceptability criteria for each SPMs are presented in tabular form as Table 6 where C_m, C_p are the measured and simulated concentration, respectively, and $\overline{A}$ denotes the mean operation of variable A.

Statistical performance of OpenFOAM results are compared with the specialised commercial code for gas dispersion FLACS in Table 6. FLACS results are extracted from (Hansen et al., 2010). The performance of current OpenFOAM code is considerably better than FLACS. In fact, FLACS is based on the porosity distributed resistance (PDR) approach. Therefore, this modelling of the boundary layer close to solid surfaces might contribute to the outperformance of the Open-

FOAM model in the comparison. In conclusion, even though larger tests were validated in FLACS, the proposed model in OpenFOAM is a promising tool for further investigation of atmospheric dense gas dispersion.

Table 6 Statistical performance measures of Hamburg unobstructed tests

SPM	MRB	RMSE	FAC2	MG	VG
Definition	$\overline{\left(\frac{C_m - C_p}{0.5(C_m - C_p)}\right)}$	$\overline{\left(\frac{(C_m - C_p)^2}{0.25(C_m + C_p)^2}\right)}$	$\frac{C_m}{C_p}$	$\exp\left(\overline{\ln \frac{C_m}{C_p}}\right)$	$\exp\left(\overline{\left(\ln \frac{C_m}{C_p}\right)^2}\right)$
Acceptable range	[-0.4,0.4]	< 2.3	[0.5, 2]	[0.67, 1.5]	< 3.3
Perfect value	0	0	1	1	1
FLACS (Hansen et al., 2010)	0.25	0.29	0.89	1.34	1.61
FOAM	-0.06	0.02	1.07	1.06	1.02

5 LNG vapour dispersion in field tests

5.1 Numerical setting

The steady simulation uses the atmospheric inlet specified by MOST. Standard $k-\epsilon$ with modifications is used to study the ability to simulate the ABL with each model. All required meteorological parameters are tabulated in Table 7, where u_{ref} and T_{ref} are air velocity and temperature at the height of 2 m respectively.

The transient simulation is divided into two steps. The first step is during the spill duration, i.e. from the time of zero to when the spill ends. The second step is after the spill stops to the end time of simulation . The gas inlet is treated as a ground boundary in this later step.

The gas inlet condition is usually obtained from separate source term modelling. There is not much information about the vaporisation of LNG from the ex-

perimental data. Therefore, uncertainty arises at the setting of this condition. Mass flux of LNG or the LNG vaporization rate is used to derive source term of LNG spilling. Luketa-Hanlin et al. (2007) reviewed a number of experiments conducted to estimate the LNG vaporization rate of the spill on water, the range of this value varied between approximately 0.029 to 0.195 $\mathrm{kg\,m^{-2}\,s^{-1}}$. In the case of Burro test, the simulated vaporisation rate is assumed to be $m''_{LNG} = 0.167\,\mathrm{kg\,m^{-2}\,s^{-1}}$. Density of LNG vapour is similar to that of CH_4 at boiling point $\rho_{LNG} = 1.76\,\mathrm{kg\,m^{-3}}$ (Luketa-Hanlin et al., 2007). The spill diameter is derived from the vaporization rate, reported spill mass m_{spill} and duration t_{spill}:

$$D_{spill} = \sqrt{\frac{4m_{spill}}{\pi m''_{LNG} t_{spill}}} \tag{18}$$

The volume spill rate is used as gas inlet condition:

$$\dot{V}_{spill} = \frac{m_{spill}}{\rho_{LNG} t_{spill}} \tag{19}$$

The LNG spill variables used in simulation are also tabulated in Table 7.

Table 7 `Burro9` tests meteorological and gas release parameters

Parameters	u_{ref}	u_*	z_0	T_{ref}	t_{spill}	D_{spill}	$\dot{V}_{spill}$
Unit	m/s	m	m/s	K	s	m	$\mathrm{m^3/s}$
	5.7	0.252	2E-4	308.55	79	32.2	77.17

5.2 Results and discussion of LNG vapour dispersion

5.2.1 The steady simulation

Profiles of velocity and turbulence quantities are sampled at the `outlet` boundary and compared with Monin-Obukhov theory profiles which are used as inlet boundary conditions. The steady state simulation of ABL with $k-\epsilon$ reveals that wind velocity and turbulence profiles are accurately reproduced as presented in Figure 7. The success of the modified $k-\epsilon$ model proves that the proposed model can adequately reproduce the Monin-Obukhov ABL profiles in the full scale simulation.

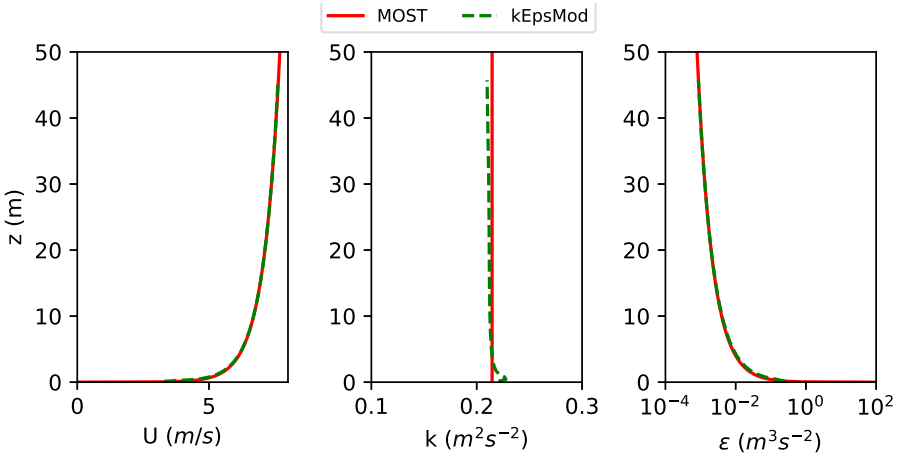

Fig. 7 Comparing ABL profiles at outlet boundary of `Burro9` simulation using modified $k-\epsilon$ model (kEpsMod) and MOST inlet profiles (MOST)

5.2.2 Mesh sensitivity study

Maximum concentration at the arcs of 57 m, 140 m, 400 m and 800 m downwind are used as performance parameters for the mesh sensitivity study. Three meshes

317 with refined factors as summarised in Table 8 are used to simulate LNG gas dis-
318 persion under adiabatic thermal wall condition. Results from four peak arc-wise
319 concentrations are plotted in Figure 8.

Table 8 Burro test computational domain and mesh parameters

	Mesh 1	Mesh 2	Mesh 3
Domain region	[(-150, 0, 50), (850, 300, 50)]		
Refined region	[(-100, 0, 5) , (400, 100, 5)]		
Mesh size (m)	10	5	2
Mesh refined size (m)	5	2	1

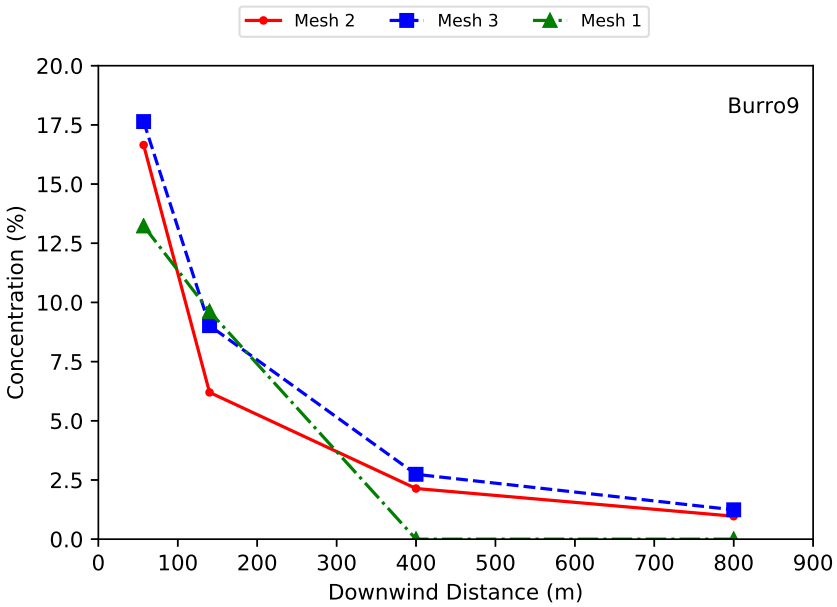

Fig. 8 Result of `Burro9` mesh sensitivity study

320 Increasingly mesh refinements help to resolve maximum concentration more
321 accurately. The difference of gas concentrations between meshes are significantly

reduced with refinement. Due to computational restriction, no further mesh is used for mesh sensitivity study and Mesh 3 parameters (Table 8) is chosen for the following study.

5.2.3 Ground heat transfer sensitivity study

Three different models of heat transfer from the ground are used to study their effect on the numerical results, which are summarised in Table 9. For constant heat flux case, the value of $200\,\mathrm{W/m^2}$ is used.

Table 9 Wall thermal boundary conditions in Burro tests

	Case 1	Case 2	Case 3
Heat transfer model	Adiabatic wall	Constant Heat Flux	Wall temperature
Label (Fig. 9)	Adiabatic	fixedFlux	fixedTem

The effect of ground heat in predicting peak gas concentration is plotted in Figure 9.

The adiabatic case results in a better prediction of experimental data than the fixed flux and fixed temperature cases. However, all simulations yield under-predicted results. This may be due to that the buoyancy effect is over-predicted and consequently the gas concentration is zero in the fixed flux case at downwind arcs (at 400 and 800 m).

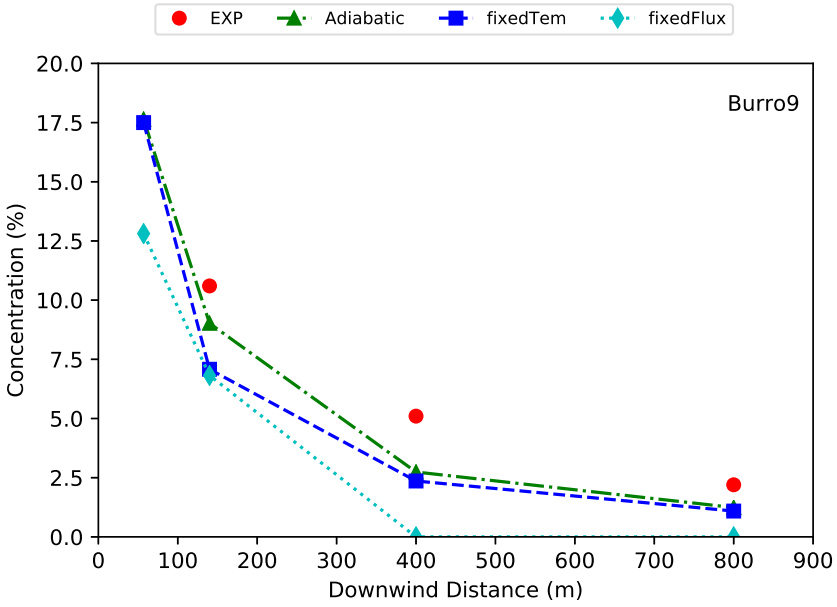

Fig. 9 Result of `Burro9` ground heat transfer study

5.2.4 Turbulence Schmidt number, Sc_t, sensitivity study

Two values of $Sc_t = 1$ and $Sc_t = 0.3$ are used for studying the sensitivity of the proposed model in predicting the maximum gas concentration. Results are compared in Figure 10.

$Sc_t = 0.3$, which was used previously in wind tunnel dense gas dispersion is shown to be appropriate for accurate prediction of maximum gas concentration at the 57 m array and 140 m array. Further downwind, at 400 m array and 800 m array, there is no significant difference between the two values.

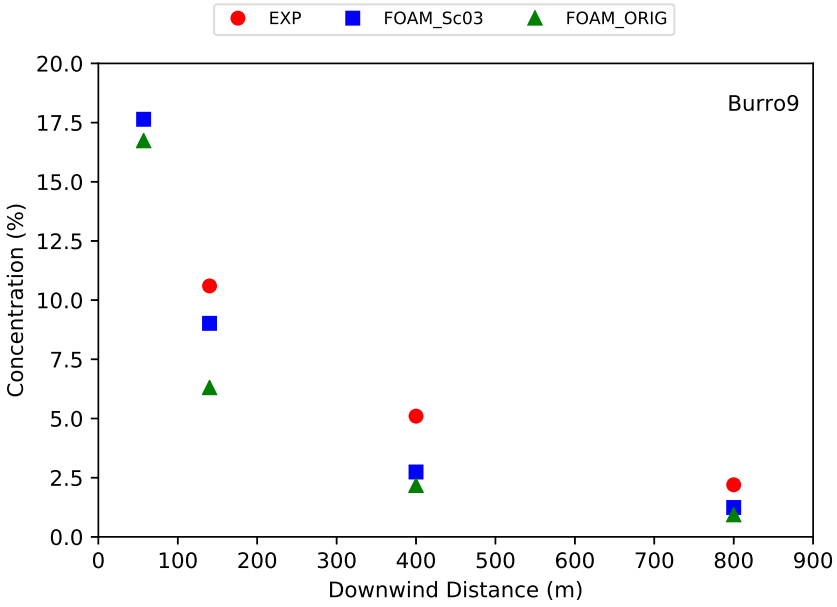

Fig. 10 Result of `Burro9` turbulent Schmidt number Sc_t study

5.2.5 Isosurface contour

The vertical isosurface contours at $X = 140$ are illustrated in Figure 11. Under-predicted cloud height are revealed in all tests indicating that the cloud buoyancy is not correctly solved.

Horizontal isosurface contours at height Z = 1 are shown in Figure 12. The gas concentration contour is plotted side by side with the contour from experiment data, where the left is the result of interpolating concentration at some concentration data points (presented in plots by black dot points), the right is from experimental data. Overall, the cloud height is considerably well predicted but the cloud width is over-predicted. Furthermore, it can be seen that the gas moves downwind slower than experimental data, which under-estimates the downwind spreading of the gas cloud.

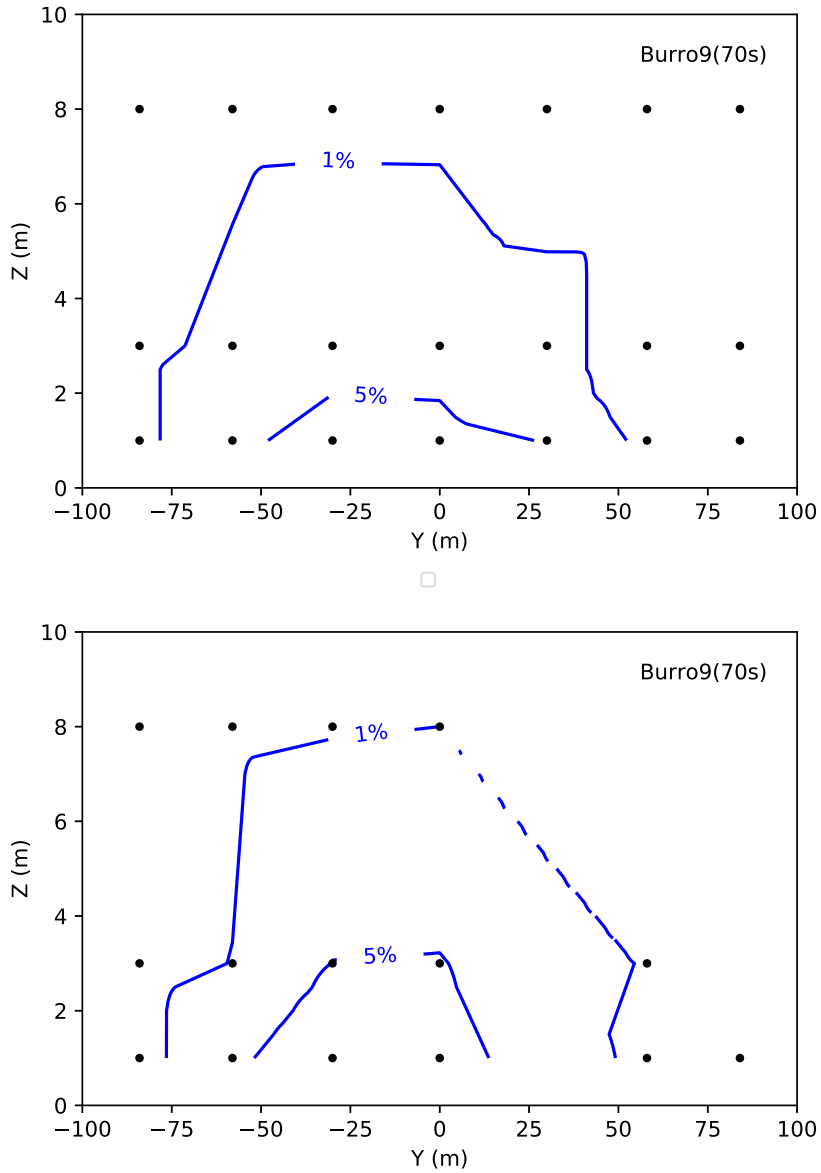

Fig. 11 Vertical isosurface at X = 140, Top: Simulation, Bottom: Experimental data of `Burro9` test

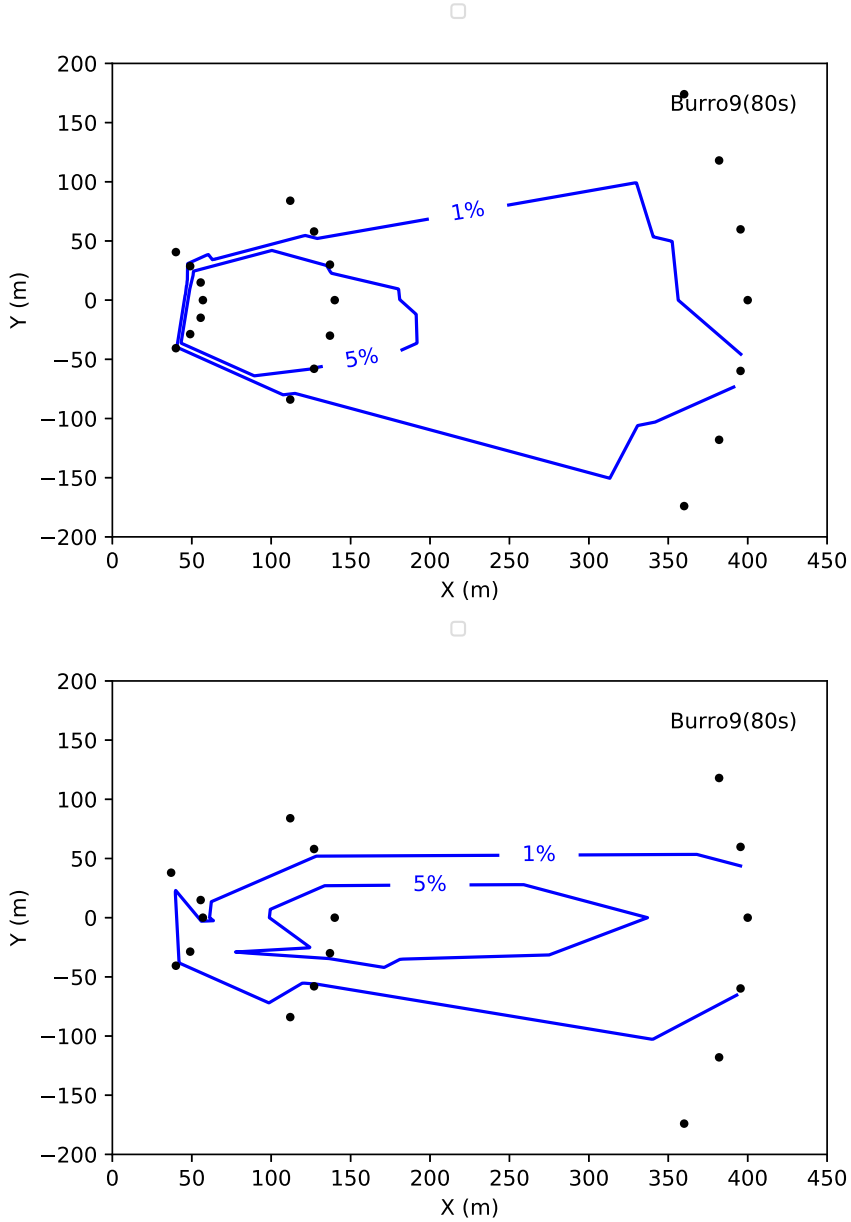

Fig. 12 Horizontal isosurface at Z = 1; Top: Simulation, Bottom: Experimental data of `Burro9` test

5.2.6 Concentration predictions

FDS (Fire Dynamics Simulator) (McGrattan et al., 2013) is a low Mach number code using the LES turbulence model. The computational domain is discretised into a connected rectilinear mesh. The governing equations are discretised using finite-difference method. A second-order scheme is used for space discretisation and an explicit second-order Runge-Kutta scheme for time discretisation. OpenFOAM concentration results are compared with FDS data extracted from (Mouilleau and Champassith, 2009).

The comparison of OpenFOAM, FDS, and experimental results for `Burro9` test is shown in Figure 13. FDS is over-predicted, while OpenFOAM is under-predicted. However, OpenFOAM is accurate in prediction at 800 m arc.

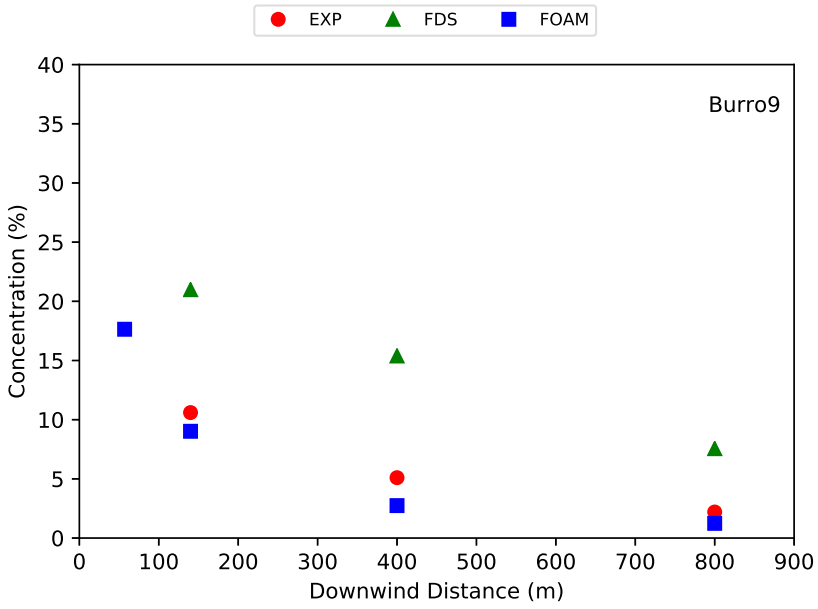

Fig. 13 Maximum arc-wise gas concentrations `Burro9` test

Figure 14 is the plot of gas concentration at 1 m elevation at 140 m downwind of `Burro9` experiment (EXP) and simulations using the developed solver (FOAM) and FDS (FDS). For the developed solver result, the peak concentration is under-estimated while the temporal trend of changing concentration generally shows good agreement with validation data. The concentration magnitude is fairly matched except during local maximum/minimum durations. Also shown in Figure 14 is the result from FDS simulation which is generally over-predicted. However, the developed solver cannot capture the fluctuation, while FDS yields fluctuating gas concentration over the time period. This is an advantage of LES over RANS turbulence model. The over-prediction of FDS may be due to that a constant coefficient Smagorinsky model was adopted in the simulation. However, the dynamic Smagorinsky model was shown to improve the gas dispersion prediction (Ferreira Jr. and Vianna, 2016). This indicates that it would be a promising approach to use LES in order to enhance the performance of the developed solver.

5.2.7 Statistical model evaluation

Overall statistical performance of OpenFOAM results are compared versus FLACS with data extracted from (Hansen et al., 2010) in Table 10. The predictions do not match all SPMs. However, some important SPMs are within the acceptable range. All gas concentrations are within a factor of two (FAC2=1) and better than FLACS (FAC2 = 0.94).

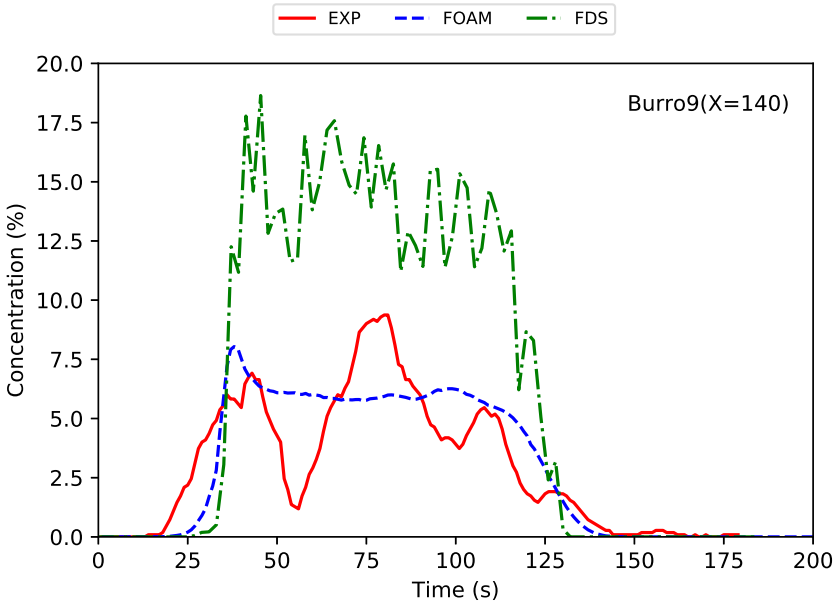

Fig. 14 Point concentration at 140 m of `Burro9` test

Table 10 Statistical performance measures of Burro tests

	MRB	RMSE	FAC2	MG	VG
FLACS (Hansen et al., 2010)	0.16	0.12	0.94	1.18	1.14
FOAM `Burro9`	0.44	0.23	1	0.63	1.28

6 Conclusions

A solver is developed to reproduce horizontal homogeneous atmospheric surface layer in neutrally stratified ABL using OpenFOAM. The empirical atmospheric boundary layer model MOST is used to specify the inlet boundary conditions for velocity, turbulent kinetic energy and dissipation rate. Flow variable profiles at outlet boundary are successfully maintained and consistent with their profiles at the inlet boundary. This demonstrates the effectiveness of the solver in simulating

the horizontal homogeneous atmospheric surface layer. It can also predict different levels of ABL turbulence kinetic energy.

A solver for ABL gas dispersion simulation taking into account buoyancy effect, variable turbulence Schmidt number and ground heat transfer is developed using the OpenFOAM platform. In the study of dense gas dispersion in neutral simulated ABL, the model is successfully validated by reproducing maximum gas concentration. SPMs from simulation results are better than those from the specialized commercial software for gas dispersion, FLACS.

In the study of LNG accidental release, a dense cold gas vapour dispersion in ABL with three ground heat transfer assumptions are simulated and compared with the full scale field measurements. The gas peak concentration is used as validation parameters. Adiabatic wall assumes zero heat flux from ground to the gas cloud, whereas, the fixed temperature model assumes isothermal ground where the ground temperate remains unchanged when in contact with the cold gas cloud. The real heat flux to the gas cloud would be in between these two cases. The other model assuming a fixed flux of heat to the gas cloud is also included. Of the three ground heat transfer models, adiabatic wall gives the closest prediction of gas peak concentration. The model is shown to accurately predict vertical buoyancy while the cloud spreading downwind is under-predicted. SPMs from the simulation results are compared with the LES code FDS and specialized dispersion code FLACS, showing that the solver is more accurate in predicting gas concentration in neutrally stratified ABL. Further investigation is required to validate the OpenFOAM solver in ABL with thermal stratification.

References

Ferreira Jr ES, Vianna SSV (2016) LARGE EDDY SIMULATION COMBINED WITH EQUIVALENT DIAMETER FOR TURBULENT JET MODELLING AND GAS DISPERSION

Fiates J, Vianna SSV (2016) Numerical modelling of gas dispersion using OpenFOAM. Process Safety and Environmental Protection 104, Part:277–293, DOI http://doi.org/10.1016/j.psep.2016.09.011, URL http://www.sciencedirect.com/science/article/pii/S0957582016302105

Fiates J, Santos RRC, Neto FF, Francesconi AZ, Simoes V, Vianna SSV (2016) An alternative CFD tool for gas dispersion modelling of heavy gas. Journal of Loss Prevention in the Process Industries 44:583–593, DOI 10.1016/j.jlp.2016.08.002, URL https://www.scopus.com/inward/record.uri?eid=2-s2.0-84994155203&doi=10.1016%2Fj.jlp.2016.08.002&partnerID=40&md5=f15971c9c9332b320e618d86adf80351

Flores F, Garreaud R, Muñoz RC (2013) CFD simulations of turbulent buoyant atmospheric flows over complex geometry: Solver development in OpenFOAM. Computers & Fluids 82:1–13, DOI http://dx.doi.org/10.1016/j.compfluid.2013.04.029, URL http://www.sciencedirect.com/science/article/pii/S0045793013001795

Foken T (2006) 50 Years of the Monin–Obukhov Similarity Theory. Boundary-Layer Meteorology 119(3):431–447, DOI 10.1007/s10546-006-9048-6, URL https://doi.org/10.1007/s10546-006-9048-6

Greenshields CJ (2017) OpenFOAM user guide version 5. URL https://cfd.direct/openfoam/user-guide/

Hansen OR, Gavelli F, Ichard M, Davis SG (2010) Validation of FLACS against experimental data sets from the model evaluation database for LNG vapor dispersion. Journal of Loss Prevention in the Process Industries 23(6):857–877, DOI 10.1016/j.jlp.2010.08.005, URL http://dx.doi.org/10.1016/j.jlp.2010.08.005

Hargreaves D, Wright N (2007) On the use of the k-epsilon model in commercial CFD software to model the neutral atmospheric boundary layer. Journal of Wind Engineering and Industrial Aerodynamics 95(5):355–369, DOI 10.1016/j.jweia.2006.08.002, URL http://www.sciencedirect.com/science/article/pii/S016761050600136X http://linkinghub.elsevier.com/retrieve/pii/S016761050600136X

Ivings MJ, Lea CJ, Webber DM, Jagger SF, Coldrick S (2013) A protocol for the evaluation of LNG vapour dispersion models. Journal of Loss Prevention in the Process Industries 26(1):153–163, DOI 10.1016/j.jlp.2012.10.005, URL http://dx.doi.org/10.1016/j.jlp.2012.10.005

Jonathon S, Christian M (2012) k-epsilon simulations of the neutral atmospheric boundary layer: analysis and correction of discretization errors on practical grids. International Journal for Numerical Methods in Fluids 70(6):724–741, DOI doi:10.1002/fld.2709, URL https://doi.org/10.1002/fld.2709

Jones WP, Launder BE (1972) The prediction of laminarization with a two-equation model of turbulence. International Journal of Heat and Mass Transfer 15(2):301–314, DOI https://doi.org/10.1016/0017-9310(72)90076-2, URL http://www.sciencedirect.com/science/article/pii/0017931072900762

Launder BE, Spalding DB (1974) The numerical computation of turbulent flows. Computer Methods in Applied Mechanics and Engineering 3(2):269–289, DOI http://dx.doi.org/10.1016/0045-7825(74)90029-2, URL

http://www.sciencedirect.com/science/article/pii/0045782574900292

Luketa-Hanlin A, Koopman RP, Ermak DL (2007) On the application of computational fluid dynamics codes for liquefied natural gas dispersion. Journal of Hazardous Materials 140(3):504–517, DOI 10.1016/j.jhazmat.2006.10.023

Mack A, Spruijt MPN (2013) Validation of OpenFoam for heavy gas dispersion applications. Journal of Hazardous Materials 262:504–516, DOI 10.1016/j.jhazmat.2013.08.065

McGrattan K, Hostikka S, McDermott R, Floyd J, Weinschenk C, Overholt K (2013) Fire dynamics simulator, user's guide. NIST special publication 1019:20

Mouilleau Y, Champassith A (2009) CFD simulations of atmospheric gas dispersion using the Fire Dynamics Simulator (FDS). Journal of Loss Prevention in the Process Industries 22(3):316–323, DOI https://doi.org/10.1016/j.jlp.2008.11.009, URL http://www.sciencedirect.com/science/article/pii/S0950423008001496

Nielsen M, Ott S (1996) A collection of data from dense gas experiments. Tech. rep., Risø National Laboratory, Roskilde

Parente A, Gorlé C, van Beeck J, Benocci C (2011) Improved k–epsilon model and wall function formulation for the RANS simulation of ABL flows. Journal of Wind Engineering and Industrial Aerodynamics 99(4):267–278, DOI https://doi.org/10.1016/j.jweia.2010.12.017, URL http://www.sciencedirect.com/science/article/pii/S016761051100002X

Pontiggia M, Derudi M, Busini V, Rota R (2009) Hazardous gas dispersion: A CFD model accounting for atmospheric stability classes. Journal of hazardous materials 171(1-3):739–747, DOI 10.1016/j.jhazmat.2009.06.064, URL http://www.sciencedirect.com/science/article/pii/S0304389409009844

Richards PJ, Hoxey RP (1993) Appropriate boundary conditions for computational wind engineering models using the k-epsilon turbulence model. Journal of Wind Engineering and Industrial Aerodynamics 46-47(Supplement C):145–153, DOI https://doi.org/10.1016/0167-6105(93)90124-7, URL http://www.sciencedirect.com/science/article/pii/0167610593901247

Richards PJ, Norris SE (2011) Appropriate boundary conditions for computational wind engineering models revisited. Journal of Wind Engineering and Industrial Aerodynamics 99(4):257–266, DOI https://doi.org/10.1016/j.jweia.2010.12.008, URL http://www.sciencedirect.com/science/article/pii/S0167610510001418

Yan BW, Li QS, He YC, Chan PW (2016) RANS simulation of neutral atmospheric boundary layer flows over complex terrain by proper imposition of boundary conditions and modification on the k-epsilon model. Environmental Fluid Mechanics 16(1):1–23, DOI 10.1007/s10652-015-9408-1

Yang Y, Gu M, Chen S, Jin X (2009) New inflow boundary conditions for modelling the neutral equilibrium atmospheric boundary layer in computational wind engineering. Journal of Wind Engineering and Industrial Aerodynamics 97(2):88–95, DOI http://dx.doi.org/10.1016/j.jweia.2008.12.001, URL http://www.sciencedirect.com/science/article/pii/S0167610508001815

CFD simulation of dense gas dispersion in neutral atmospheric boundary layer with OpenFOAM

Tran, Vu

2019-08-02

Tran V, Ng EYK, Skote M. (2019) CFD simulation of dense gas dispersion in neutral atmospheric boundary layer with OpenFOAM. Meteorology and Atmospheric Physics, Volume 132, April 2020, pp. 273–285

https://doi.org/10.1007/s00703-019-00689-2